J Supercond Nov Magn
DOI 10.1007/s10948-017-4241-z

LETTER

Filamentary Superconductivity in Semiconducting Policrystalline $ZrSe_2$ Compound with Zr Vacancies

Gabriela Tenorio[1,2] · L. Bucio[2] · R. Escudero[1,2]

Received: 1 July 2017 / Accepted: 6 July 2017

Abstract $ZrSe_2$ is a band semiconductor studied long time ago. It has interesting electronic properties, and because its layer structure can be intercalated with different atoms to change some of the physical properties. In this investigation, we found that Zr deficiencies alter the semiconducting behavior and the compound can be turned into a superconductor. In this paper, we report our studies related to this discovery. The decreasing of the number of Zr atoms in small proportion according to the formula Zr_xSe_2, where x is varied from about 8.1 to 8.6 K, changing the semiconducting behavior to a superconductor with transition temperatures ranging between 7.8 and 8.5 K, is depending on the deficiencies. Outside of those ranges, the compound behaves as semiconducting with the properties already known. In our experiments, we found that this new superconductor has only a very small fraction of superconducting material determined by magnetic measurements with applied magnetic field of 10 Oe. Our conclusions is that superconductivity is filamentary. However, in one studied sample, the fraction was about 10.2 %, whereas in others is only about 1% or less. We determined the superconducting characteristics; the critical fields that indicate a type 2 superonductor with Ginzburg-Landau κ parameter of the order about 2.7. The synthesis procedure is quite normal following the conventional solid state reaction. In this paper, included are the electronic characteristics, transition temperature, and evolution with temperature of the critical fields.

Keywords Superconductivity · Filamentary superconductivity · Semiconductors

1 Introduction

$ZrSe_2$ crystalizes in C6-CdI_2 type structure. Frequently may exhibits deviations of stoichiometry, that changes it physical properties. Many of those studies were performed many years ago by Van Arkel, MacTaggart and Wadsley, Han and Ness, Gleitzes and Jeannin [1–4]. The crystalline structure of $ZrSe_2$ has a chain-like structure formed by a sequence of stacking atoms in the unit cell, In Fig. 1, we show the structure of this compound with details related to vacancies and stacking of the structure. As mentioned by these authors, the variant of stacking atoms in C6 type compounds may present vacancies of Se or Zr depending on the Se/Zr ratio, the crystal structure of the compound has parallel layers consisting of two hexagonal chalcogenes planes with one hexagonal Zr plane. The intralayer bonds are strong, whereas the others are quite weak. The compound is highly anisotropic as seen in its physical properties, i.e., electrical and thermal conductivity, as many other properties [5]. In fact, it is important to mention that defects in $ZrSe_2$, play an important role in the compound, as Gleitzes and Jeannin found [4]. They observed that two types of defects or vacancies can occur depending on the Se/Zr ratio. One important change we found is related to the semiconducting behavior to superconducting character. These new characteristics reported here are the main result of our investigations. Thus, we found that decreasing the Zr content up to some small level $ZrSe_2$ becomes a type 2 superconductor.

✉ R. Escudero
escu@unam.mx

[1] Instituto de Investigaciones en Materiales, Universidad Nacional Autónoma de México, Apartado Postal 70-360, México, D.F. 04510, México

[2] Instituto de Física, Universidad Nacional Autónoma de México, México, D.F. 04510, México

Published online: 13 July 2017

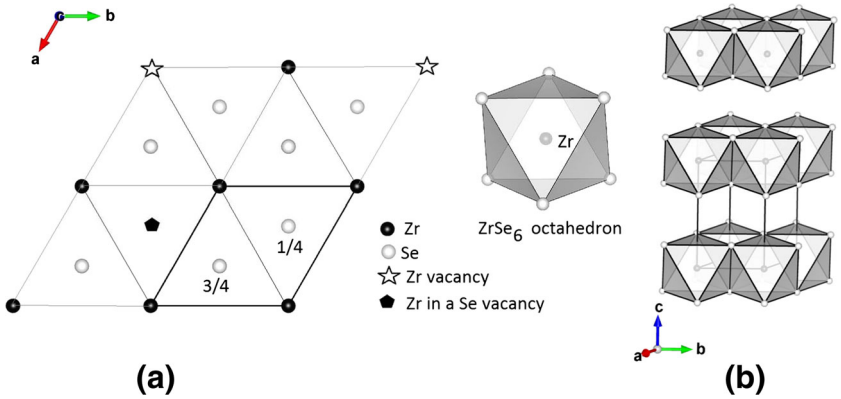

Fig. 1 (Color on-line) Crystalline structure of $ZrSe_2$ and deficiencies. In **a**, we show Zr in Se positions, **b** shows the stacking structure of the compound, in the middle is shown the $ZrSe_6$ octhahedron. This stacking structure permits the intercalation of small atoms

2 Experimental Details

Synthesis of the $ZrSe_2$ was carried out by solid state reactions. Zr and Se reactives were alpha Aldrich with purities of 99.9 and 99.999%, respectively. The powders were mixed in an agatha mortar inside a globe box. The powders with appropriated stoichiometry were sealed in a quartz tube under a clean atmosphere free of oxygen using first, an argon atmosphere, and evacuated. The synthesize was performed at a temperature of 800 °C in different periods of time. In general, we noted that 5 or 6 days of heating is enough to obtain a pure compound. Several samples with different stoichiometries, Zr_xSe_2, were produced. The amount of Zr content was changed from $x = 0.70$ to 0.97 according to the formula Zr_xSe_2. In these two limits, the resulting compound is semiconducting, whereas in between the material becomes superconducting with small variation in the transition temperature.

Chemical analysis for all samples was performed by Rutherford backscattering spectrometry (RBS) performed using a Pelletron NEC accelerator (National Electrostatics Corp, Middleton, WI) with 3 MeV beam of alpha particles. RBS spectra were collected with a detector at an angle of 12° respect to the incident beam. The sample surface was normal to the incident beam. Experimental chemical analysis was fitted to a theoretically calculated curve by means of the program XRUMP.

3 X-ray Diffraction Analysis and Structural Characterization

Powders of each sample for X-ray determination were measured at room temperature in a Bruker D8 Advance diffractometer (Bruker AXS GmbH, Karlsruhe, Germany; $CuK_{\alpha 1}$ radiation, $\lambda = 1.5405$ Å and goniometer with a lynx-eye detector (Bruker AXS GmbH). Data were collected from 2θ, 6–90°, with 30 kV and 40 mA in the X-ray generator. Figure 2 displays X-ray data and analyses by Rietveld. The structural information for each one of the identified phases was obtained from the Inorganic Crystal Structure Database (ICSD) databank [6]. Cell parameters, crystal symmetry, and atomic coordinates were introduced in the Rietveld program GSAS [7] using the graphical interphase EXPGUI [8]. A modified pseudo-Voigt function was chosen to generate the peak shapes of the diffraction reflections. The refined parameters were zero point and scale factors, cell parameters, half-width, preferred orientation, and atomic occupancy factors. Two types of defects proposed by Gleizes and Jeannin [4] for the $ZrSe_2$ structure were considered in the Rietveld refinements.

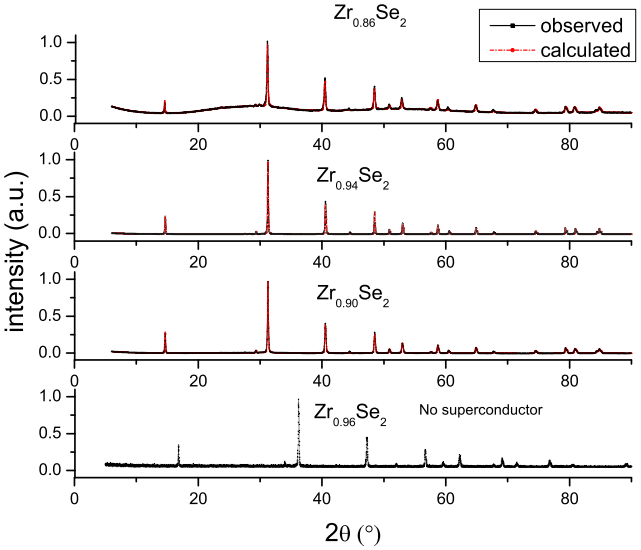

Fig. 2 (Color on-line) Difractograms of four samples and compositions, the bottom difractogram with maximum Zr content about 0.96% was not superconducting. The three next difractograms with Zr content 0.90, 0.94, and 0.86 were superconducting. The crystalline structure was Rietveld refined and shows complete agreements to $ZrSe_2$ close to the stoichiometric composition, without impurities. Slightly above 0.94. the compound is semiconducting. The *small black dots* in the figures are the observed data, and the *red lines* are the Riettveld fitting

4 Results and Discussion

Single phase of $ZrSe_2$ was found in all samples with exception of the sample with high superconducting fraction about 10.3%, where selenium appears as secondary phase. This is shown in the first column of table. In the crystallographic data for $ZrSe_2$ reported by Van Arkel [1], Zr is at the origin of the unit cell, while Se occupies the 2d position at (1/3, 2/3, 1/4) forming a layered structure, details are clearly shown in Fig. 1. Each layer has a sandwich-like structure in which Zr atoms form a two-dimensional hexagonal close packing plane and six Se atoms octahedrally coordinate each of them (Fig. 1b). Of the two types of defects proposed by Gleizes and Jeannin [4], only one (that refers to vacancies of Zr atoms, located at the origin of the unit cell) led to good results in our Rietveld refinements; however, as mentioned by Ikari et al. [9], Zr also may be found in interticial site of the crystal structure. The second type of defect has to do with substitution of Se by Zr in the (1/3, 2/3, 1/4) position; since in the refinements the occupancy factors for Se and Zr gave practically 1 and 0, respectively, this defect was considered absent in the samples. With this dominant defect, we found that the lattice parameters vary from 3.7722 to 3.7576 $\AA$ for a, and from 6.1297 to 6.135 $\AA$ for c, as the Se/Zr ratio increases from 2.06 to 2.47 and the superconducting fraction increases from 0 to 10.3% as shown in (Table).

The crystal structure was determined by X-ray diffraction analysis and the structural characterization of the powders of each sample at room temperature with a Bruker D8 Advance diffractometer (Bruker AXS GmbH, Karlsruhe, Germany; using Cu$K_{\alpha 1}$ radiation, $\lambda = 1.5405$ $\AA$ and goniometer with a lynx-eye detector (Bruker AXS GmbH). Data were collected, in 2θ from 6 to 90°, with 30 kV and 40 mA in the X-ray generator. A glass sample holder was used to perform the characterization of powders. The X-ray analysis and structural characterization information for each sample was obtained and identified using the ICSD databank (see Table). Cell parameters, crystal symmetry, and atomic coordinates were introduced to fit the crystal structure using Rietveld program. It is interesting to mention that cell parameters determined for this compound coincides with calculation of other authors, see for instances Reshak et al. [10]. A modified pseudo-Voigt function was chosen to generate the peak shapes of reflections. The refined parameters were zero point and scale factors, cell parameters, half-width, atomic coordinates, isotropic thermal coefficients for each phase. For the case of the $ZrSe_2$ vacancies, there were considered in the Zr sites and the occupancy of this site was refined.

5 Superconducting Characteristics

Figures 3 and 4 show the superconducting behavior of the compounds. Figure 3 displays four curves of magnetization-temperature of four different samples with different Zr vacancies, the four samples show small variation of the transition critical temperature but clearly defined from 8.14, 8.31, 8.34, and 8.59 onsets in Kelvins. Those curves were determined in ZFC an FC in order to determine the fraction of superconductivity. In Fig. 4, we present the behavior of the two critical fields.

As before mentioned, one important aspect on this study is related to defects configuration in the crystalline structure

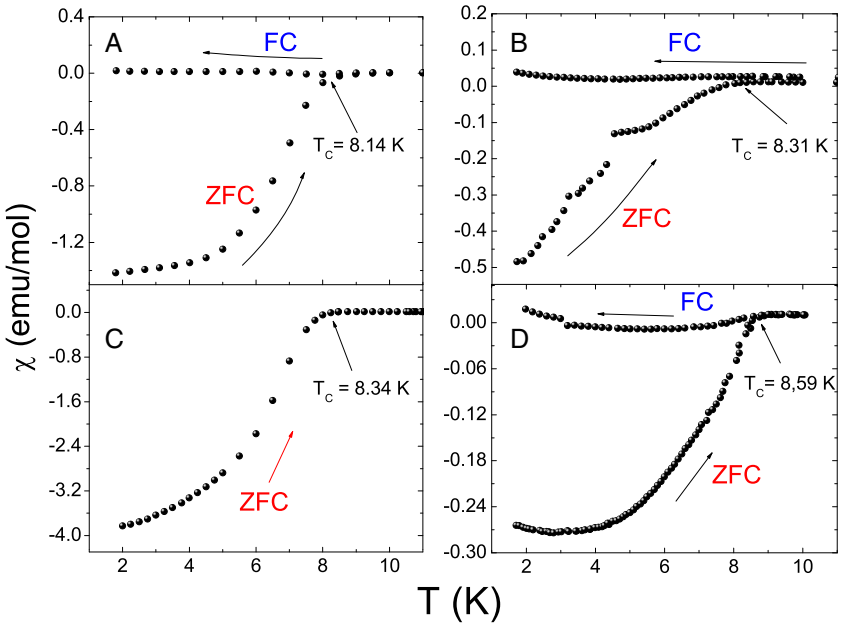

Fig. 3 (Color on-line) Superconducting transition temperature determined by magnetic measurements with field of 10 Oe in two modes of measurements, zero field cooling (ZFC) and field cooling (FC). The *curves* show small differences in transition temperature but appreciables. *Arrows* mark the onset temperature from 8.14, 8.31, 8.34, and 8.59 K. The fraction of superconducting material was very small, only in Fig C the amount was about 10.2%, others were about 1% or small

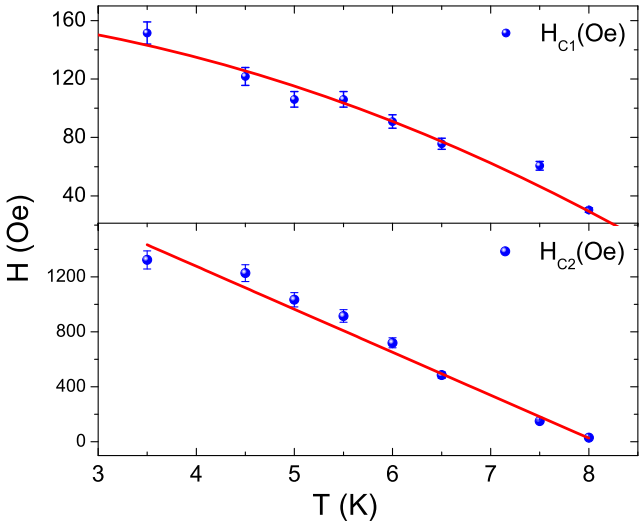

Fig. 4 (Color on-line) Critical magnetic fields H_{C1}, and H_{C2} versus temperature. H_{C1} at the lower temperature is about 170 Oe, whereas H_{C2} is about 2400 Oe. H_{C1} fits quite well to a parabolic behavior with transition temperature at 8.8 K, but the best fit for H_{C2} was a linear function

of the compound. The defects on the (100) plane, as found by Gleizes and Jeannin, [4] is quite important because some of the physical properties are depending on it, for instance in the Se/Zr ratio. The number of defects (vacancies) is a critical aspects for the physics behavior; the number of defects (vacancies) is important and turn to be very complicated in elucidation of the involved physics. The electronic properties depend of the missing atom and position on the cell. The superconducting characteristics also are depending on the number of vacancies. According to this, the compound, could be semiconductor, metal, or superconductor.

Onuki et al. [12] and Thompson [13] have studied the electrical properties of TiS_2 and $ZrSe_2$; they found that in T^2, the resistivity behavior, above 50 K, behaves as a degenerated semiconductor similarly as occurs in $ZrSe_2$. This is a consequence that the number of defects change the size of the band gap. Our Fig. 5 shows a similar picture of the distribution of vacancies in the (100) plane, considering only Zr atoms as our compositions; with Zr vacancies about 0.75, 0.80, and 0.85, this figure is quite similar to in the Gleizes and Jeannin paper. It is worth mentioning that in Onuki et al. [11, 12], they mention similar deficiencies in the TiS_2. The changes on the density of states is depending on the number of missing Ti atoms, and therefore physical properties displays a change from a weak metallic behavior to a semiconductor and to a metal. In our study, Zr deficiencies provoke a change into the t_{2g} band. This is our main consideration to the change from semiconducting to a superconductor. It is important to mention that in this compound, six valence bands are primarily derived from Se $4p$ orbitals while the conduction bands are derived from the Zr $4d$ orbitals [14, 15]. It is worth mentioning the importance of the band filling in the compound: the six valence bands of this compound are primarily derived from chalcogen p orbitals while the conduction bands are derived from the transition metal d orbitals. The valence band can hold 12 electrons per unit cell, so after filling the valence band, no d electrons remain for TiS_2 and $ZrSe_2$, making them semiconductors with indirect band gaps, e.g., 0.2 eV and 1 eV, respectively. Klipstein et al. [16] found that TiS_2 is a degenerate semiconductor which carriers do not arise from p, d band overlap, but from partial occupation of t_2g band resulting by Ti excess. and the compound becomes a degenerated semiconductor and the high conductivity can be attributed

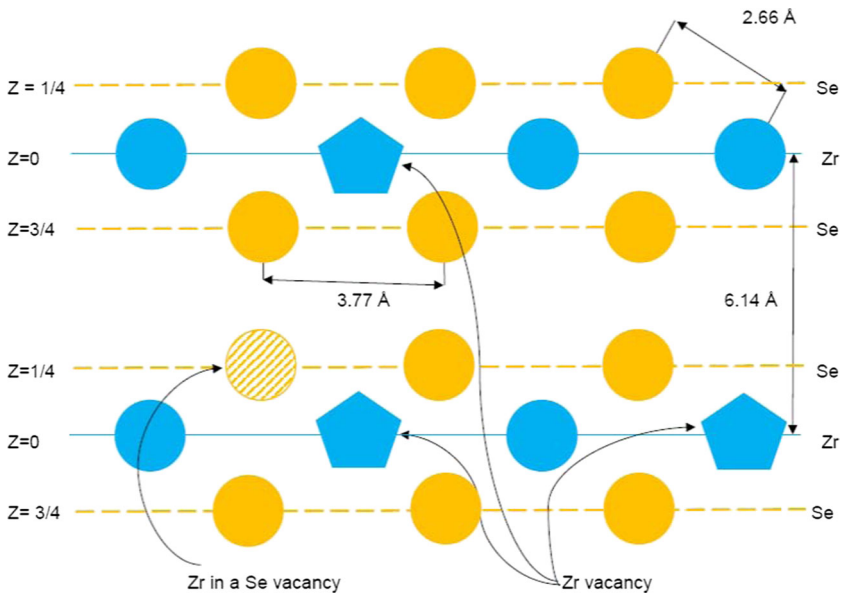

Fig. 5 (Color on-line) Possible defects or vacancies configuration in Zr_xSe_2 with deficiencies of Zr, according to Gleizes and Jeannin analyzes [4]. *Blue circles* correspond to Zr atoms, Se are in *yellow* color. Vacancies can be in different sites and number

Table 1 Table shows the characteristics of the studied samples

Samples	S1		S2	S3	S4
Superconducting fraction (%)	10.3		1.3	0.7	0.0
Crystal phases	$Zr_{0.81}Se_2$	Se	$Zr_{0.93}Se_2$	$Zr_{0.93}Se_2$	$Zr_{0.97}Se_2$
ICSD code*	652244	53801	652244	652244	652244
Weight (%)	99.76(5)	0.24(4)	100	100	100
Space group	P-3m1	$P3_121$	P-3m1	P-3m1	P-3m1
Cell parameters ($\AA$)	$a = 3.7576(6)$	$a = 4.40(1)$	$a = 3.7695(1)$	$a = 3.7701(2)$	$a = 3.7722(3)$
	$c = 6.135(1)$	$c = 4.948(9)$	$c = 6.1437(2)$	$c = 6.1354(4)$	$c = 6.1297(4)$
Volume ($\AA$3)	75.01(3)	83.0(4)	75.60(1)	75.52(1)	75.54(1)
Se/Zr ratio**	2.47		2.15	2.15	2.06
Zr/Se ratio***	2.44		1.54	2.38	1.54
R_{wp}	0.038		0.064	0.113	0.109
R_p	0.028		0.043	0.082	0.074

Samples S1, S2, and S3 are superconducting, sample S4 is not. Table shows the detected phases, the ICSD code, space group, and cell parameters; only in S1 we see a drastic reduction of volume. The details were determined by Rietveld analyses. However, the most important change related to superconductivity was the proportion of ZrSe ratio. The main phase was modeled with the structural type of $ZrSe_2$, code in the ICSD database listed in the table. Those number were **calculated from the quantification of identified phases by Rietveld refinement, and ***calculated from RBS results

to charge transfer from self intercalated Ti atoms in the Van der Waals interlayer space.

As mentioned by Brauer et al. [11, 12], they investigate an interesting behavior related to the band filling in TiS_2. The band structure of the valence band can hold 12 electrons per unit cell, and no electrons remain after filling; thus, TiS_2 and $ZrSe_2$ becomes semiconducting, with a band gap about 1 to 1.3 eV. The six valence bands are primarily derived from chalcogen p orbitals while the conduction bands are derived from the transition metal d orbitals. The valence band can hold 12 electrons per unit cell, so after filling the valence band, no d electrons remain for TiS_2 and $ZrSe_2$, making them semiconductors with indirect band gaps, e.g., once the band is not completed filled with the Zr vacancies, then superconductivity characteristic arises. In other situations, the compound behaves as a semiconductor.

It is important to mention that the superconducting characteristics show only a small diamagnetic fraction, so the superconductivity fraction is very small, or we can call filamentary. In Fig. 2, we show those measurements, in plots of magnetization-temperature, (M-T) determined in zero field cooling (ZFC) and field cooling (FC) at 10 Oe. Figure 3 shows the critical fields, top figure shows HC_1 fitted to a parabolic function with critical temperature of $T_C = 8.8$ K. Bottom plot displays HC_2. fitted only to a linear function. The magnitude of the two critical fields is of the order of 170, and 2500 Oe for the two fields. The superconductor is a type 2, with thermodynamic field about $HC = 650$ Oe, so the the Ginzburg-Landau parameter, κ is 2.70, is in the strong coupling limit [17]. In order to have more insight into the characteristics of this new superconductor, various samples were used to measure the specific heat in function of temperature, close to the superconducting temperature, we never see the specific heat jump related to the transition. This is clearly indicative that the superconductivity is only a very small fraction, and therefore filamentary. Resitivity meaurements were not measured, because the compound was powder, and almost impossible to form a bulk compact material (Table 1).

6 Conclusions

We have found and studied a new superconducting compound with composition $ZrSe_2$, which presents a transition temperature about 8.14–8.59 K with Zr vacancies from about 0.75, 0.8, and 0.85, out of this small window range the semiconducting compound is as already determined.

Acknowledgments We thank to DGAPA UNAM project IT106014, and to A. López-Vivas, and A. Pompa-García (IIM-UNAM) for help in technical problems.

References

1. Van Arkel, A.E.: Physica **4**, 286 (1924)
2. MacTaggart, K.F., Wadsley, A.D.: Australian J. Chem. **II**, 445 (1958)
3. Han, H., Ness, P.: Naturwiss **44**, 534 (1957)
4. Gleitzes, A., Jeannin, Y.: J. Solid State Chem. **1**, 180 (1970)

5. Isomaki, H., von Bohem, J.: Phys. Scr. **24**, 465 (1981)
6. ICSD: Inorganic Crystal Structure Database. Fachinformations zentrum Karlsruhe, and the U.S Secretary of Commerce on behalf of the United States (2013)
7. Larson, A.C., Von Dreele, R.B.: General Structure Analysis System, GSAS. Los Alamos National Laboratory Report LAUR 86748 (2000)
8. Toby, B.H.: EXPGUI, a graphical user interface for GSAS. J. Appl. Cryst. **34**, 210–213 (2001)
9. Ikari, T., Maeda, K., Futagami, Nakashima, A.: Jpn. J. Appl. Phys. **34**, 1442 (1995)
10. Reshak, A.H., Auluck, S.: Phys. B **353**, 230–237 (2004)
11. Onuki, Y., Inada, R., Tanuma, S.: J. Phys. Soc. Jpn. **51**(4), 1223 (1982)
12. Onuki, Y. et al.: Synth. Met. **5**, 245–255 (1983)
13. Thompson, A.H.: Phys. Rev. Lett. **35**, 1786 (1975)
14. Brauer, H.E. et al.: J. Phys.: Condens. Matter **6**, 7741 (1995)
15. Brauer a, H.E., Starnberg, H.I., Holleboom, L.J., Hughes, H.P.: Surf. Sci. **331–333**, 419–424 (1995)
16. Klipstein, P.C., Bagnall, A.G., Liang, W.Y., Marseglia, E.A., Friend, R.H.: Phys. C: Solid State Phys. **14**, 40674081 (1981). Printed in Great Britain
17. Kittel, Ch.: Introduction to Solid State Phys. Wiley, New York (1971)